Single-Antenna Coherent Detection of Collided FM0 RFID Signals

Aggelos Bletsas, *Member, IEEE*, John Kimionis, *Student Member, IEEE*, Antonis G. Dimitriou, *Member, IEEE*, and George N. Karystinos, *Member, IEEE*

***Abstract*—This work derives and evaluates single-antenna detection schemes for *collided* radio frequency identification (RFID) signals, i.e. simultaneous transmission of two RFID tags, following FM0 (biphase-space) encoding. In sharp contrast to prior art, the proposed detection algorithms take explicitly into account the FM0 encoding characteristics, including its inherent memory. The detection algorithms are derived when error at *either* or *only one* out of two tags is considered. It is shown that careful design of one-bit-memory two-tag detection can improve bit-error-rate (BER) performance by 3dB, compared to its memoryless counterpart, on par with existing art for single-tag detection. Furthermore, this work calculates the total tag population inventory delay, i.e. how much time is saved when two-tag detection is utilized, as opposed to conventional, single-tag methods. It is found that two-tag detection could lead to significant inventory time reduction (in some cases on the order of 40%) for basic framed-Aloha access schemes. Analytic calculation of inventory time is confirmed by simulation. This work could augment detection software of existing commercial RFID readers, including single-antenna portable versions, without major modification of their RF front ends.**

***Index Terms*—RFID, Gen2, FM0 coding, collision detection.**

I. Introduction

SIGNIFICANT progress has been made since the invention and first use of RFID, i.e. transmission of an identification bit string by means of signal reflection rather than active radiation [1]. Today, relevant applications have emerged in various domains, including logistics/inventory management [2], backscatter sensor networks [3]–[5], or even musical instruments [6], [7].

Anti-collision of RFIDs in the widely-used UHF industry standard EPC Class 1 Generation 2 (Gen2, also ISO-registered as $18000-6C$) [8] is based on framed-Aloha, i.e. time is split in frames and each frame in slots; tags randomize their broadcast to minimize probability of simultaneous transmission of more than one tags at a given slot [9], [10]. In other words, tag *collision* is harmful only when the RFID reader cannot detect information from more than one simultaneous tag transmissions. However, Gen2 does not specify reader detection and leaves open the possibility to exploit simultaneous tag transmissions. It is remarked that older RFID standardization attempts considered binary tree splitting methods for collision-free tag access, which were later abandoned in Gen2.

The scientific community has recently attempted to redefine the notion of RFID collision, by proposing new receiver methods that could withstand simultaneous reception of more than one tags. Work in [11] is perhaps one of the first that utilized a custom, software-defined radio monitor for RFID signals and tested separation of non-Gen2 tags with DBPSK modulation. Work in [12] tested high signal-to-noise ratio (SNR) detection methods for simultaneous reception of more than one non-Gen2 tags and was based on meticulous observation of the in-phase (I) and quadrature (Q) components of the received backscattered signal, after transmission from more than one tags. Careful modeling of the backscatter radio channel and the received I and Q components were further exploited in [13] with zero-forcing techniques. Furthermore, throughput enhancement of framed Aloha was theoretically calculated. Multi-antenna detection, based on blind source separation of zero constant-modulus signals, was proposed in [14] and experimentally validated in [15].

However, the aforementioned techniques above were either based on multi-antenna techniques or (even at the case of single-reader antenna) did not exploit the characteristics of tag transmission *encoding*, including inherent memory for the special case of FM0. Also known as biphase-space, FM0 is one of the two encoding schemes used in Gen2 tags and is broadly utilized in commercial tags (the other scheme is Miller or biphase-mark encoding).

In this work, we explicitly take into account the FM0 encoding characteristics, including its inherent memory and derive and evaluate single-antenna detection schemes for simultaneous transmission of two tags. Our developments do not assume a specific channel (or I/Q) model and were inspired from work in [16] which presented BER-optimal detection of a *single* FM0-encoded RFID tag. We follow the same signal model which is validated by experimental measurements using a custom software-defined radio receiver (sniffer). Specifically, utilization of the magnitude of the in-phase/quadrature (I/Q) signal eliminates the frequency offset between RFID reader and sniffer. Furthermore, we focus on tag population inventory delay, i.e. we compute how much time is saved when two-

Paper approved by A. Zanella, the Editor for Wireless Systems of the IEEE Communications Society. Manuscript received April 12, 2011; revised October 3, 2011.

This work was supported in part by the Ministry of National Education of Greece under Thales program grants DISCO and RFID-CORE. Material in this paper was presented at the IEEE International Conference on RFID Technologies and Applications (RFID-TA), Sitges, Spain, Sept. 2011.

A. Bletsas, J. Kimionis, and G. N. Karystinos are with the Telecommunications Laboratory, Electronic and Computer Engineering Dept., Technical Univ. of Crete, Chania 73100, Greece (e-mail: {aggelos, jkimionis, karystinos}@telecom.tuc.gr).

A. G. Dimitriou is with the Electrical and Computer Engineering Dept., Aristotle Univ. of Thessaloniki, Thessaloniki 54124, Greece (e-mail: antodimi@auth.gr).

Digital Object Identifier 10.1109/TCOMM.2011.020612.110212

tag detection is utilized as opposed to conventional single-tag detection. Inventory time is measured in slots and calculated reduction is performed through theoretic calculation and confirmed by simulation. In that way, the benefits of the proposed signal detection techniques are highlighted in the context of RFID inventory applications.

Contributions of this work are summarized below:

A. Single-antenna methods that exploit FM0 encoding are derived for two-tag detection without any specific modeling assumptions regarding the backscatter channel or reader front end (I and Q components).
B. At the physical layer, it is shown how one-bit memory of FM0 encoding can be also exploited in *two-tag* detection to improve performance by 3 dB, compared to maximum-likelihood (ML) memoryless *two-tag* detection. Analytic BER results are confirmed by simulation.
C. At the medium access control (MAC) layer, analytic results are offered regarding tag population inventory delay reduction (as opposed to throughput) for a basic version of framed-Aloha. Analysis is confirmed by simulation.

The single-antenna detection methods of this work could be readily applied in multi-antenna commercial RFID readers (e.g. Gen2), especially those that operate in antenna switching mode, without any modification of their RF front end. Furthermore, this work could enhance performance in portable RFID readers, where physical size forbids more than one antennas (especially in UHF). The proposed methods accelerate the inventory of a given tag population and their performance is quantified at both physical and MAC layers.

Section II describes the basic assumptions and formulates the problem studied in this work. Section III studies a multitude of memoryless or memory-assisted single-antenna detection methods for simultaneous transmission of *two* FM0-encoded tags. Section IV analytically calculates the overall delay (in number of slots) for inventory of many tags as a function of conventional or nonconventional (the latter are proposed in this work) reader detection policies. Finally, Sections V and VI offer the simulation results and conclusion, respectively.

II. Problem Formulation and System Model

In FM0 encoding, signal (line) level always changes at the bit boundaries. Moreover, signal level changes at the middle of the bit period only for bit “0" (while for bit “1" the level is kept constant) as depicted in Fig. 1. Thus, encoding of a single FM0 bit requires *memory* of the previous bit so that signal levels are modified accordingly at the bit boundaries. Each FM0-encoded bit can be represented as a vector of two half-bit constants of the form $[\pm a \ \ \pm a]^T$ where sign of a depends on the transmitted bit as well as the signal memory (i.e. previous transmission level).

To validate the signal model of [16] that we follow in this work, we utilized a simple and low-cost measurement setup (Fig. 2(c)) that consists of a commercial UHF Gen2 reader, two FM0 tags, and a USRP software-defined radio (SDR) with a broadband daughterboard tuned at 865 MHz; the SDR acts as a low-cost Gen2 monitor (sniffer). A SDR-based Gen2 monitor was also recently developed in [17]. With custom

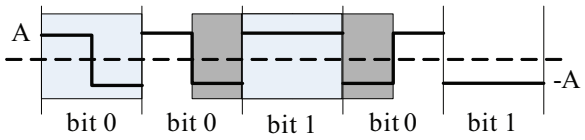

Fig. 1. Baseband FM0 signal of a single tag. Levels always change at the bit interval. For bit “0," level also changes at the middle of the bit period.

software developed throughout this work, conversation between two tags and the reader was recorded at the sniffer. The down-converted baseband signal magnitude $\sqrt{I^2(t)+Q^2(t)}$ at the sniffer (where $I(t)$ and $Q(t)$ represent the in-phase and quadrature, respectively) is depicted in Fig. 2(a) where it is shown that on top of a DC constant there is encoded information (due to the carrier transmitted from the reader and scattered back from the tags).

The signal part depicted as “collision" is magnified and zero-centered in Fig. 2(b), which depicts the measured down-converted sum of two FM0 signals; such “collision" corresponds to simultaneous transmission (through backscatter) during the *query* phase of the Gen2 protocol, when random 16-bit ID information is transmitted by each tag (a.k.a. RN16). The above measurement validates the signal model of [16] followed in this work; furthermore, processing of $\sqrt{I^2(t)+Q^2(t)}$ eliminates the frequency offset between reader and sniffer. It is noted however that at an operating RFID reader, where the detection methods proposed in this work could be implemented, there is no frequency offset between the reader’s transmit and receive paths (i.e. the reader uses the same oscillator for up- and down-conversion) [18].

Given that tag transmission (via backscatter) in commercial RFID protocols (e.g. Gen2) is always initiated and directed by the reader, while the typical range of such systems is on the order of a few meters and the minimum bit duration is on the order of a few microseconds, one would expect the two collided tag signals to arrive at the sniffer (or the reader) with negligible time difference compared to the bit duration and aligned bit boundaries. Thus, detecting such collided information is simpler than prior art that addresses separation of co-channel signals with misaligned bits. For example, one could first ignore the weak signal, detect bits from the strongest signal, remodulate it and cancel it from the aggregate received waveform in the frequency domain and then perform detection of the weakest signal (e.g. see relevant work in [19] and references therein). In this work, the fact that tags respond to reader signals in a slotted fashion is explicitly taken into account. Furthermore, the bit alignment assumption is validated by experimental measurements and the followed formulation facilitates the exploitation of the inherent memory of the FM0 line encoding. On the other hand, the amplitudes of the received tag signals also depend on the particular phases of their backscattered carrier (as well as on range from reader) and, thus, should be in general different.

Indeed, the aforementioned assumptions above are confirmed by measurements. Fig. 2(c) depicts how the *measured* signal looks from two collided FM0 tags. Similar measurement plots have also appeared in [15], [17], and [20]. One could observe four different amplitude levels stemming from the

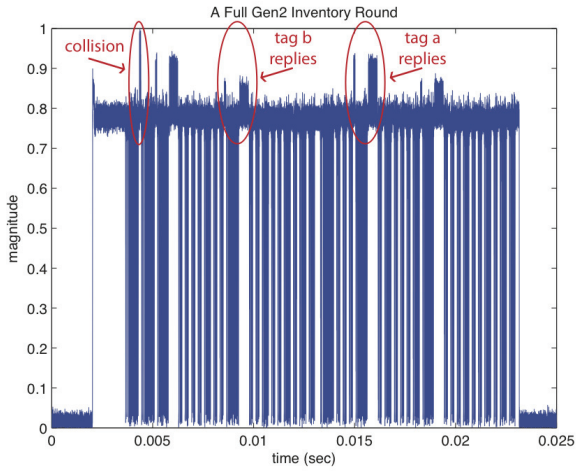

(a) Reader and two tags conversation captured at the sniffer.

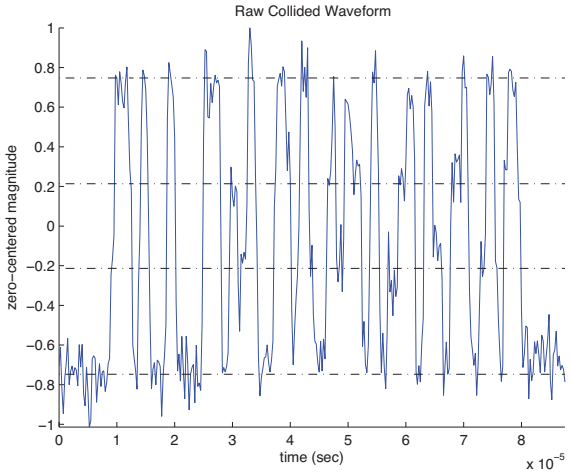

(b) Zero-centered magnitude of the received waveform for two collided FM0 tags.

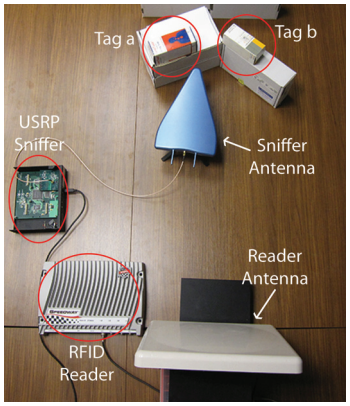

(c) The custom measurement setup.

Fig. 2. Baseband received signal at the sniffer with conversation between reader and two tags. The signal depicted as "collision" in the second figure is magnified and zero-centered in the third figure and depicts two collided FM0 signals from two tags.

addition of the two tags. There are also interesting *spikes* either due to noise or due to *bit duration* mismatch; the latter is due to the fact that RFID tags do not typically have accurate crystals for timing purposes but instead derive clocking signals from the reader-transmitted carrier through low-cost passive components with, in general, variable manufacturing tolerance [18].

Consequently, after pulse-matched filtering and sampling at the RFID reader, the in-phase (or quadrature)[1] component of the collided signal during one bit period can be represented by a vector $[x_0\ x_1]^T$ of two half-bit symbols, where each half-bit symbol belongs in $\mathcal{S} = \{s_0 = -a - b, s_1 = -a + b, s_2 = a - b, s_3 = a + b\}$. Slow fading can be assumed, i.e. $a,\ b$ remain constant during reception given the limited number of considered bits, either in RN16 or in the actual tag ID (96 bits in electronic product code). We also assume *coherent* reception, i.e. the constants $a,\ b$ are considered known at the receiver. Such knowledge can be acquired through estimation using specialized pilot signals or could be estimated by the observation of the four amplitude levels of the aggregate downconverted and filtered data. It is remarked that, if $a = b$, then $s_1 = s_2 \in \mathcal{S}$ and information is lost, i.e. separation of tags A and B fails. In general, $a \neq b$ and their power ratio will be explicitly taken into account. The power ratio of signals from two tags can easily vary by several dBs, even for equidistant tags from the reader, as experimentally measured in [21]. Tag chip mismatching and and chip variability (e.g. chips produced by different vendors) further increase the power variability of the received backscattered signals received at the reader. Without loss of generality, we assume $a > b > 0$ throughout this work.

Under the above assumptions, the received signal can be written in vector form as

$$\mathbf{y} \triangleq \begin{bmatrix} y_0 \\ y_1 \end{bmatrix} = \begin{bmatrix} x_0 \\ x_1 \end{bmatrix} + \mathbf{n} \tag{1}$$

where $[x_0\ x_1]^T \in \mathcal{S}^2$ is the collided information signal and $\mathbf{n} = [n_0\ n_1]^T$ represents additive white Gaussian noise (AWGN) where n_0, n_1 are independent, zero-mean Gaussian variables with variance σ^2.

The minimum distance (ML) rule given measurement $y_i, i \in \{0, 1\}$, and transmitted constellation $\mathcal{S}$, with decision boundaries depicted in Fig. 3, provides the following conditional

[1]For simplicity of the derivations and clarity of the presentation, in this work we consider processing of the in-phase (or quadrature) component only. Our developments can be extended to joint processing of the in-phase and quadrature components in a straightforward manner.

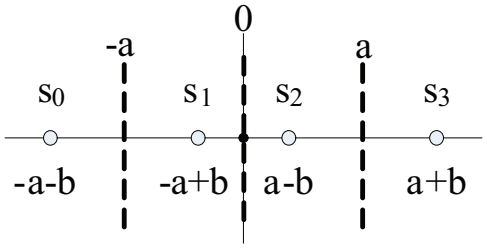

Fig. 3. The two-tag, nonuniform signal constellation with decision areas (marked with intermittent lines) based on the minimum distance rule.

error probability:

$$\begin{aligned}\Pr\left(\hat{x}_i \neq x_i | x_i = s_0\right) &= \Pr\left(\hat{x}_i \neq x_i | x_i = s_3\right) \\ &= Q\left(b/\sigma\right), \qquad i = 0, 1,\end{aligned} \tag{2}$$

$$\begin{aligned}\Pr\left(\hat{x}_i \neq x_i | x_i = s_1\right) &= \Pr\left(\hat{x}_i \neq x_i | x_i = s_2\right) \\ &= Q\left((a-b)/\sigma\right) + Q\left(b/\sigma\right), \qquad i = 0, 1,\end{aligned} \tag{3}$$

where $Q(x) = \frac{1}{\sqrt{2\pi}} \int_x^{+\infty} e^{-t^2/2} dt$ is the Q function. The expressions above will be found useful throughout the document.

The above modeling approach is sufficient for the examination of the proposed two-tag detection methods. For complex modeling of the backscatter radio channel, the interested reader could refer to several works, including [3], [13], and [22].

III. Detection Techniques

In Subsections III-A, III-B, and III-C, we derive three methods for detection of both tag A and tag B FM0 information, alongside their respective (single-bit and bit-pair) error probabilities. In Subsections III-D and III-E, two methods are derived for single-tag detection.

A. Method 1: Memoryless Detection Based on ML and Two Half-Bits

This method performs independent detection of the two half-bit symbols (according to decision areas of Fig. 3) and then, based on the findings, final decision on both tag A and B information is jointly made. The detection method is summarized below.

- Detect $\hat{x}_0 \in \mathcal{S}$ from y_0, applying a ML (i.e. minimum-distance) rule.
- Detect $\hat{x}_1 \in \mathcal{S}$ from y_1, applying a ML (i.e. minimum-distance) rule.
- Decide in favor of H_i (i.e. $\hat{\mathrm{H}} = \mathrm{H}_i$), $i \in \{0, 1, 2, 3\}$, from sign change between $\hat{x}_0$ and $\hat{x}_1$. If sign of a in $\hat{x}_0$ is different than in $\hat{x}_1$, then $\widehat{\mathrm{tag}}_\mathrm{A} = 0$, otherwise $\widehat{\mathrm{tag}}_\mathrm{A} = 1$. Similarly, if sign of b in $\hat{x}_0$ is different than in $\hat{x}_1$, then $\widehat{\mathrm{tag}}_\mathrm{B} = 0$, otherwise $\widehat{\mathrm{tag}}_\mathrm{B} = 1$.

For example, if $\hat{x}_0 = a - b = s_2$ and $\hat{x}_1 = -a - b = s_0$, then the bit estimates for tags A and B are $\mathrm{tag}_\mathrm{A} = 0$ and $\mathrm{tag}_\mathrm{B} = 1$, respectively. Such a case corresponds to hypothesis H_2 according to Table I-A. It is remarked that Method 1 does not require knowledge of the noise variance σ^2 per half-bit at the receiver.

It is straightforward to compute error (or, equivalently, zero-error) performance of the above detection method. Observing that, under hypothesis H_0 and FM0 signaling, only transitions between s_0 and s_3 or between s_1 and s_2 are allowed, the following conditional error probability can be readily calculated:

$$\begin{aligned}&\Pr(\hat{\mathrm{H}}_i, i \neq 0 | \mathrm{H}_0) = 1 - \Pr(\hat{\mathrm{H}}_0 | \mathrm{H}_0) \\ &= 1 - \frac{1}{4}\left\{\left[1 - \Pr(\hat{x}_0 \neq x_0 | x_0 = s_0)\right]\left[1 - \Pr(\hat{x}_1 \neq x_1 | x_1 = s_3)\right]\right. \\ &\quad + \left[1 - \Pr(\hat{x}_0 \neq x_0 | x_0 = s_1)\right]\left[1 - \Pr(\hat{x}_1 \neq x_1 | x_1 = s_2)\right] \\ &\quad + \left[1 - \Pr(\hat{x}_0 \neq x_0 | x_0 = s_2)\right]\left[1 - \Pr(\hat{x}_1 \neq x_1 | x_1 = s_1)\right] \\ &\quad \left. + \left[1 - \Pr(\hat{x}_0 \neq x_0 | x_0 = s_3)\right]\left[1 - \Pr(\hat{x}_1 \neq x_1 | x_1 = s_0)\right]\right\} \\ &= 1 - \frac{1}{2}\left\{\left[1 - Q(b/\sigma)\right]^2 + \left[1 - Q(b/\sigma) - Q((a-b)/\sigma)\right]^2\right\}.\end{aligned} \tag{4}$$

Under hypothesis H_1 and FM0 signaling, transitions between s_0 and s_1 or between s_2 and s_3 are allowed. Thus,

$$\begin{aligned}&\Pr(\hat{\mathrm{H}}_i, i \neq 1 | \mathrm{H}_1) = 1 - \Pr(\hat{\mathrm{H}}_1 | \mathrm{H}_1) \\ &= 1 - \frac{1}{4}\left\{\left[1 - \Pr(\hat{x}_0 \neq x_0 | x_0 = s_0)\right]\left[1 - \Pr(\hat{x}_1 \neq x_1 | x_1 = s_1)\right]\right. \\ &\quad + \left[1 - \Pr(\hat{x}_0 \neq x_0 | x_0 = s_1)\right]\left[1 - \Pr(\hat{x}_1 \neq x_1 | x_1 = s_0)\right] \\ &\quad + \left[1 - \Pr(\hat{x}_0 \neq x_0 | x_0 = s_2)\right]\left[1 - \Pr(\hat{x}_1 \neq x_1 | x_1 = s_3)\right] \\ &\quad \left. + \left[1 - \Pr(\hat{x}_0 \neq x_0 | x_0 = s_3)\right]\left[1 - \Pr(\hat{x}_1 \neq x_1 | x_1 = s_2)\right]\right\} \\ &= 1 - \left\{\left[1 - Q(b/\sigma)\right]\left[1 - Q(b/\sigma) - Q((a-b)/\sigma)\right]\right\}.\end{aligned} \tag{5}$$

Under similar reasoning, it can be shown that

$$\Pr(\hat{\mathrm{H}}_i, i \neq 2 | \mathrm{H}_2) = \Pr(\hat{\mathrm{H}}_i, i \neq 1 | \mathrm{H}_1), \tag{6}$$

$$\Pr(\hat{\mathrm{H}}_i, i \neq 3 | \mathrm{H}_3) = \Pr(\hat{\mathrm{H}}_i, i \neq 0 | \mathrm{H}_0). \tag{7}$$

Therefore, the probability of detection error in *at least* one of the two tags is given by

$$\begin{aligned}&\Pr\left(\widehat{(\mathrm{tag}_\mathrm{A}, \mathrm{tag}_\mathrm{B})} \neq (\mathrm{tag}_\mathrm{A}, \mathrm{tag}_\mathrm{B})\right) = \frac{1}{4}\sum_{j=0}^{3} \Pr(\hat{\mathrm{H}}_i, i \neq j | \mathrm{H}_j) = \\ &= Q\left(\frac{b}{\sigma}\right)\left[2 - Q\left(\frac{b}{\sigma}\right) - Q\left(\frac{a-b}{\sigma}\right)\right] \\ &\qquad + Q\left(\frac{a-b}{\sigma}\right)\left[1 - \frac{1}{4}Q\left(\frac{a-b}{\sigma}\right)\right].\end{aligned} \tag{8}$$

If we restrict the definition of detection error *solely* with respect to tag A, i.e. correct (or erroneous) detection of tag B is indifferent, and follow Method 1, then the error probability can be also readily calculated. Decision areas for half-bit detection in Fig. 3 become ($y_i < 0$ for $\hat{x}_i = s_0$ or s_1 and $y_i > 0$ for $\hat{x}_i = s_2$ or s_3, $i \in \{0, 1\}$) and conditional error probabilities of eqs. (2) and (3) are modified to

$$\begin{aligned}\Pr(\hat{x}_i = s_2 \text{ or } s_3 | x_i = s_0) &= \Pr(\hat{x}_i = s_0 \text{ or } s_1 | x_i = s_3) \\ &= Q\left(\frac{a+b}{\sigma}\right), \qquad i = 0, 1,\end{aligned} \tag{9}$$

$$\begin{aligned}\Pr(\hat{x}_i = s_2 \text{ or } s_3 | x_i = s_1) &= \Pr(\hat{x}_i = s_0 \text{ or } s_1 | x_i = s_2) \\ &= Q\left(\frac{a-b}{\sigma}\right), \qquad i = 0, 1.\end{aligned} \tag{10}$$

Following the same derivation of eqs. (4)-(7), the bit error probability of detection of tag A information with Method 1

becomes

$$\Pr(\widehat{\text{tag}}_{\text{A}} \neq \text{tag}_{\text{A}}) = \left[Q\left(\frac{a+b}{\sigma}\right) + Q\left(\frac{a-b}{\sigma}\right)\right] \times \left\{1 - \frac{1}{4}\left[Q\left(\frac{a+b}{\sigma}\right) + Q\left(\frac{a-b}{\sigma}\right)\right]\right\}. \quad (11)$$

B. Method 2: ML Memoryless Detection

The previous method performs optimal hard decision per half-bit and then decides in favor of the detected hypothesis based on the half-bit hard decisions. In the following, we base our decision directly on the entire bit duration (without making half-bit decisions) and derive the ML detection rule. It is reminded that x_0 denotes the first half-bit symbol.

Under hypothesis H_0, both tags change their signal levels after the end of the first half-bit. Thus, signal $a+b$ becomes $-a-b$, signal $a-b$ becomes $-a+b$, and so forth. As a result, the conditional pdf of the received two-sample vector becomes

$$\begin{aligned} f(\mathbf{y}|\text{H}_0) &= \frac{1}{4}\sum_{j=0}^{3} f(\mathbf{y}|\text{H}_0, x_0 = s_j) \\ &= \frac{1}{4}g(-a-b, a+b) + \frac{1}{4}g(a-b, -a+b) \\ &\quad + \frac{1}{4}g(a+b, -a-b) + \frac{1}{4}g(-a+b, a-b) \\ &= k_2\ e^{-\frac{2ab}{\sigma^2}} \cosh\left[\frac{(a+b)(y_1-y_0)}{\sigma^2}\right] \\ &\quad + k_2\ e^{+\frac{2ab}{\sigma^2}} \cosh\left[\frac{(a-b)(y_1-y_0)}{\sigma^2}\right] \quad (12) \end{aligned}$$

where k_2 is a positive term and $g(a_0, a_1) \triangleq \mathcal{N}([\begin{smallmatrix} a_0 \\ a_1 \end{smallmatrix}], \sigma^2\mathbf{I}_{2\times 2}; [\begin{smallmatrix} y_0 \\ y_1 \end{smallmatrix}])$. The other three conditional pdfs are calculated similarly and equal

$$\begin{aligned} f(\mathbf{y}|\text{H}_1) &= k_2\ \cosh\left[\frac{(a-b)y_0 - (a+b)y_1}{\sigma^2}\right] \\ &\quad + k_2\ \cosh\left[\frac{(a+b)y_0 - (a-b)y_1}{\sigma^2}\right], \quad (13) \end{aligned}$$

$$\begin{aligned} f(\mathbf{y}|\text{H}_2) &= k_2\ \cosh\left[\frac{(a+b)y_0 + (a-b)y_1}{\sigma^2}\right] \\ &\quad + k_2\ \cosh\left[\frac{(a-b)y_0 + (a+b)y_1}{\sigma^2}\right], \quad (14) \end{aligned}$$

$$\begin{aligned} f(\mathbf{y}|\text{H}_3) &= k_2\ e^{+\frac{2ab}{\sigma^2}} \cosh\left[\frac{(a-b)(y_0+y_1)}{\sigma^2}\right] \\ &\quad + k_2\ e^{-\frac{2ab}{\sigma^2}} \cosh\left[\frac{(a+b)(y_0+y_1)}{\sigma^2}\right]. \quad (15) \end{aligned}$$

Notice that the above expressions require knowledge of σ^2. Thus, the ML detector is given by

$$\hat{\text{H}} = \underset{\text{H}\in\{\text{H}_0,\text{H}_1,\text{H}_2,\text{H}_3\}}{\arg\max} \{f(\mathbf{y}|\text{H})\}. \quad (16)$$

Although, given knowledge of σ^2 at the receiver, Method 2 outperforms Method 1 in terms of BER by definition, the two detectors' error probabilities *practically* coincide with each other, as will be demonstrated with results. Such observation holds when bit-pair error probability (i.e. both tags) as well as when single-bit error probability (i.e. tag A only) is of interest. Such result can be explained by the fact that the two half-bit observations of Method 1 constitute sufficient statistics for memoryless detection and hence performance in not degraded compared to Method 2. It is stressed however that Method 2 requires knowledge of the noise variance σ^2, while Method 1 does not.

C. Method 3: One-Bit-Memory-Assisted Detection

The previous two methods focus on the duration of a single bit (two consecutive half-bits) and, therefore, did not exploit the inherent memory of FM0 signaling. In Method 3, memory of FM0 signaling is exploited in detection of two collided FM0 signals by observing duration of *exactly two* bits: the bit under observation, half-bit before it, and half-bit after it. Similar mind-set was exploited by Simon and Divsalar [16] for detection of a *single* tag. They noticed that for ML single-bit (memoryless) detection there are four possible hypotheses to test; however, if half-bit before and half bit after are also observed, then there are only two hypotheses at the bit boundary (see shaded half-bits at Fig. 1). Below, we extend the idea in detection and separation of *two* FM0 tags.

With slight abuse of notation, we denote by y_0 the received half-bit signal before the bit boundary and y_1 the received half-bit signal after the bit boundary. Thus, there is a pair of measurements $(y_0, y_1)^0$ where y_1 corresponds to the first half-bit and y_0 corresponds to the second half-bit of the previous bit and a second pair of measurements $(y_0, y_1)^1$ where y_0 corresponds to the second half-bit and y_1 corresponds to the first half-bit of the next bit.

Given that the FM0 signal of each tag always changes levels at the bit boundaries, the possible transmitted symbols s_0, s_1, s_2, and s_3 under either pair of measurements $(y_0, y_1)^i, i = 0, 1$, are depicted in Figs. 4(a) and 4(b). The detection algorithm works as follows:

- Detect $\hat{x}_0 \in \mathcal{S}$ from $(y_0, y_1)^0$, applying a ML (i.e. minimum-distance) rule (Fig. 4(a)).
- Detect $\hat{x}_1 \in \mathcal{S}$ from $(y_0, y_1)^1$, applying a ML (i.e. minimum-distance) rule (Fig. 4(b)).
- Decide in favor of $\text{H}_i, i = 0, 1, 2, 3$, based on $\hat{x}_0, \hat{x}_1$, according to Table I-B.

For example, if $\hat{x}_0 = s_2$ (Fig. 4(a)) and $\hat{x}_1 = s_0$ (Fig. 4(b)), then tag B level remains constant at $= -b$ (i.e. bit "1") while tag A level switches from $+a$ to $-a$ (i.e. bit "0"). Thus, we decide in favor of hypothesis H_2, according to Table I-bottom. Similarly, the other entries above can be worked out.

The ML (i.e. minimum-distance) rule for $(y_0, y_1)^0$ or $(y_0, y_1)^1$ can be directly derived. Working on $(y_0, y_1)^0$ and $(y_0, y_1)^1$, the distances for the four transmitted symbols s_0, s_1, s_2, s_3 are given by d_0^i, d_1^i, d_2^i, and d_3^i, $i = 0, 1$, respectively, that are equal to

$$d_0^0[y_0, y_1] = d_3^1[y_0, y_1] = [y_0 - (a+b)]^2 + [y_1 - (-a-b)]^2, \quad (17)$$

$$d_1^0[y_0, y_1] = d_2^1[y_0, y_1] = [y_0 - (a-b)]^2 + [y_1 - (-a+b)]^2, \quad (18)$$

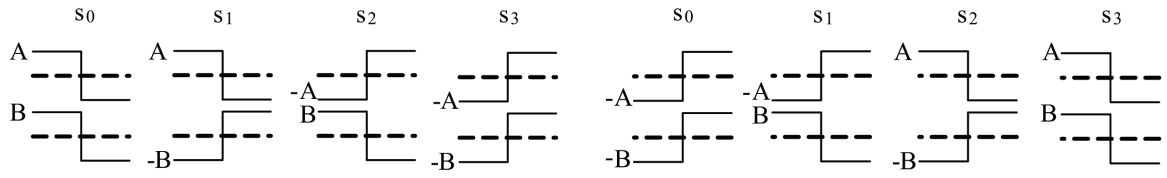

(a) Waveform constellation of x_0. (b) Waveform constellation of x_1.

Fig. 4. Transmitted symbols for the first (left) and second (right) pairs of measurements in memory-assisted detection.

TABLE I

	H_0	H_1	H_2	H_3
tag_A	0	1	0	1
tag_B	0	0	1	1

$\hat{x}_0$	s_0	s_0	s_0	s_0	s_1	s_1	s_1	s_1	s_2	s_2	s_2	s_2	s_3	s_3	s_3	s_3
$\hat{x}_1$	s_0	s_1	s_2	s_3	s_0	s_1	s_2	s_3	s_0	s_1	s_2	s_3	s_0	s_1	s_2	s_3
$\hat{H}$	H_3	H_1	H_2	H_0	H_1	H_3	H_0	H_2	H_2	H_0	H_3	H_1	H_0	H_2	H_1	H_3

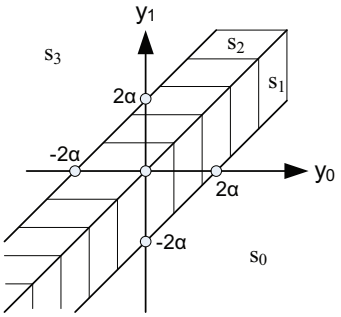

Fig. 5. Decision areas for each pair of measurements in memory-assisted detection.

$$d_2^0[y_0,y_1] = d_1^1[y_0,y_1] = [y_0-(-a+b)]^2 + [y_1-(a-b)]^2, \tag{19}$$

$$d_3^0[y_0,y_1] = d_0^1[y_0,y_1] = [y_0-(-a-b)]^2 + [y_1-(a+b)]^2. \tag{20}$$

Using $(y_0,y_1)^0$ and the distances of d_0^0, d_1^0, d_2^0, and d_3^0, in the following we describe how decision on $\hat{x}_0$ is made. Similar approach is followed subsequently for the decision on $\hat{x}_1$ (based on $(y_0,y_1)^1$ and d_0^1, d_1^1, d_2^1, and d_3^1).

We detect $\hat{x}_0 = s_0$ if and only if

$$d_0^0 < d_1^0 \Leftrightarrow y_0 - y_1 > 2a, \tag{21}$$

$$d_0^0 < d_2^0 \Leftrightarrow y_0 - y_1 > 2b, \tag{22}$$

$$d_0^0 < d_3^0 \Leftrightarrow y_0 - y_1 > 0. \tag{23}$$

Having in mind that $a > b$, we obtain

$$\hat{x}_0 = s_0: \quad y_0 - y_1 > 2a. \tag{24}$$

Working similarly for the other three hypotheses of Fig. 4(a), corresponding to the bit boundary with the previous bit, the ML decision areas become

$$\hat{x}_0 = \begin{cases} s_0, & y_0 - y_1 > 2a, \\ s_1, & 0 < y_0 - y_1 < 2a, \\ s_2, & -2a < y_0 - y_1 < 0, \\ s_3, & y_0 - y_1 < -2a. \end{cases} \tag{25}$$

The four decision areas above are depicted in Fig. 5.

Following similar steps for the hypotheses of Fig. 4(b), corresponding to the bit boundary with the next bit, we can derive the corresponding decision rules for $\hat{x}_1$ (based on $(y_0,y_1)^1$ and d_0^1, d_1^1, d_2^1, and d_3^1) which are simplified to:

$$\hat{x}_1 = \begin{cases} s_0, & y_0 - y_1 < -2a, \\ s_1, & -2a < y_0 - y_1 < 0, \\ s_2, & 0 < y_0 - y_1 < 2a, \\ s_3, & y_0 - y_1 > 2a. \end{cases} \tag{26}$$

Erroneous detection of tag A or tag B FM0 signals occurs when detection from $(y_0,y_1)^0$ *or* detection from $(y_0,y_1)^1$ fails. The conditional error probabilities of such a detection scheme can be readily calculated. For example, the conditional error probability, given that $x_0 = s_0$, equals

$$\Pr(\hat{x}_0 \neq x_0 | x_0 = s_0) = \int_{y_0=-\infty}^{\infty} \int_{y_1=y_0-2a}^{\infty} f(y_0,y_1|x_0=s_0)\, dy_1 dy_0 \tag{27}$$

$$= \int_{y_0=-\infty}^{\infty} \int_{y_1=y_0-2a}^{\infty} g(a+b,-a-b) dy_1 dy_0. \tag{28}$$

The other three conditional error probabilities

$$\Pr(\hat{x}_0 \neq x_0 | x_0 = s_1), \Pr(\hat{x}_0 \neq x_0 | x_0 = s_2)$$

and

$$\Pr(\hat{x}_0 \neq x_0 | x_0 = s_3)$$

can be expressed similarly.

The above method requires numerical integration of the Q function. However, carefully observing that the method above improves the signal energy by exactly a factor of 2, since duration of two bits is exploited, as opposed to memoryless (single-bit) Method 1, it is inferred that the error performance of Method 3 improves over Method 1 with a SNR factor of two. Therefore, the probability $\Pr(\widehat{(\text{tag}_\text{A}, \text{tag}_\text{B})} \neq (\text{tag}_\text{A}, \text{tag}_\text{B}))$ that *at least* one of the two tag information is erroneously detected with Method 3 is given by

$$\Pr(\widehat{(\text{tag}_\text{A}, \text{tag}_\text{B})} \neq (\text{tag}_\text{A}, \text{tag}_\text{B})) = Q\left(\sqrt{2}\,\frac{b}{\sigma}\right)\left[2 - Q\left(\sqrt{2}\,\frac{b}{\sigma}\right) - Q\left(\sqrt{2}\,\frac{a-b}{\sigma}\right)\right] + Q\left(\sqrt{2}\,\frac{a-b}{\sigma}\right)\left[1 - \frac{1}{4}\,Q\left(\sqrt{2}\,\frac{a-b}{\sigma}\right)\right]. \tag{29}$$

Simulation results confirm the calculated expression above.

Furthermore, if detection of tag A information is important while tag B detected bits can be ignored, then the performance of Method 3 can also be calculated. Following the same reasoning as above, BER performance $\Pr(\widehat{\text{tag}}_{\text{A}} \neq \text{tag}_{\text{A}})$ of Method 3, when only tag A is of interest, is given by Eq. (11) with SNR improved by a factor of 2:

$$\Pr(\widehat{\text{tag}}_{\text{A}} \neq \text{tag}_{\text{A}}) = \left[Q\left(\sqrt{2}\,\frac{a+b}{\sigma}\right) + Q\left(\sqrt{2}\,\frac{a-b}{\sigma}\right)\right] \times \left\{1 - \frac{1}{4}\left[Q\left(\sqrt{2}\,\frac{a+b}{\sigma}\right) + Q\left(\sqrt{2}\,\frac{a-b}{\sigma}\right)\right]\right\}. \quad (30)$$

Numerical results confirm that the above expression coincides with simulation results. It is remarked that Method 3 does not require knowledge of the noise variance σ^2.

The previous Methods $1-3$ targeted detection at both tags, even though performance was also calculated when only tag A was of interest. In the following subsections, ML detectors are derived when only tag A information is of interest (in the presence of tag B), with or without single-bit memory.

D. Method 4: ML Memoryless Single-Tag Detection

Working similarly as before, with x_0, x_1 the first and second half-bit and hypotheses in $\mathcal{S}$ of Fig. 3, the conditional pdfs are given by

$$\begin{aligned} &f(\mathbf{y}|\text{tag}_{\text{A}} = \text{“0”}) \\ &= \frac{1}{8}\sum_{i=0}^{3} f(\mathbf{y}|\text{tag}_{\text{A}} = \text{“0”}, \text{tag}_{\text{B}} = \text{“0”}, x_0 = s_i) \\ &\qquad + \frac{1}{8}\sum_{i=0}^{3} f(\mathbf{y}|\text{tag}_{\text{A}} = \text{“0”}, \text{tag}_{\text{B}} = \text{“1”}, x_0 = s_i) \quad (31) \\ &= k_4 \Big(e^{-\frac{2ab}{\sigma^2}} \cosh\left[(a+b)(y_0 - y_1)/\sigma^2\right] \\ &\qquad + e^{+\frac{2ab}{\sigma^2}} \cosh\left[(a-b)(y_0 - y_1)/\sigma^2\right] \\ &\qquad + \cosh\left\{\left[a(y_0 - y_1) + b(y_0 + y_1)\right]/\sigma^2\right\} \\ &\qquad + \cosh\left\{\left[a(y_0 - y_1) - b(y_0 + y_1)\right]/\sigma^2\right\}\Big) \quad (32) \end{aligned}$$

and

$$\begin{aligned} &f(\mathbf{y}|\text{tag}_{\text{A}} = \text{“1”}) \\ &= \frac{1}{8}\sum_{i=0}^{3} f(\mathbf{y}|\text{tag}_{\text{A}} = \text{“1”}, \text{tag}_{\text{B}} = \text{“0”}, x_0 = s_i) \\ &\qquad + \frac{1}{8}\sum_{i=0}^{3} f(\mathbf{y}|\text{tag}_{\text{A}} = \text{“1”}, \text{tag}_{\text{B}} = \text{“1”}, x_0 = s_i) \quad (33) \\ &= k_4 \Big(e^{-\frac{2ab}{\sigma^2}} \cosh\left[(a+b)(y_0 + y_1)/\sigma^2\right] \\ &\qquad + e^{+\frac{2ab}{\sigma^2}} \cosh\left[(a-b)(y_0 + y_1)/\sigma^2\right] \\ &\qquad + \cosh\left\{\left[a(y_0 + y_1) + b(y_0 - y_1)\right]/\sigma^2\right\} \\ &\qquad + \cosh\left\{\left[a(y_0 + y_1) - b(y_0 - y_1)\right]/\sigma^2\right\}\Big) \quad (34) \end{aligned}$$

where k_4 is a positive term, common to both hypotheses. It is remarked that the above expressions require knowledge of σ^2 at the receiver.

The receiver simply decides $\widehat{\text{tag}}_{\text{A}} = \text{“0”}$ iff

$$f(\mathbf{y}|\text{tag}_{\text{A}} = \text{“0”}) > f(\mathbf{y}|\text{tag}_{\text{A}} = \text{“1”}),$$

and $\widehat{\text{tag}}_{\text{A}} = \text{“1”}$ otherwise. Numerical results show that the performance of such detector practically can coincide with the performance of Method 1 (Eq. (11)).

E. Method 5: One-Bit-Memory-Assisted Single-Tag Detection

Finally, a single-bit memory-assisted detector is derived, when only tag A is of interest. Similarly to Method 3, we work separately on $(y_0, y_1)^0$ (corresponding to bit boundary with the previous bit) and $(y_0, y_1)^1$ (corresponding to bit boundary with the next bit) and decide in favor of hypotheses M^0 and M^1, respectively, where $\text{M}^i, i = 0, 1$, can be either M_0 (that corresponds to constellation signals s_0, s_1 of Fig. 4(a)) or M_1 (that corresponds to constellation signals s_2, s_3 of Fig. 4(a)). Considering ML detection of $\hat{\text{M}}^0$ from $(y_0, y_1)^0$, we utilize the conditional pdfs

$$f\left((y_0, y_1)^0|\text{M}_0\right) = \frac{1}{2}f\left((y_0, y_1)^0|s_0\right) + \frac{1}{2}f\left((y_0, y_1)^0|s_1\right), \quad (35)$$

$$f\left((y_0, y_1)^0|\text{M}_1\right) = \frac{1}{2}f\left((y_0, y_1)^0|s_2\right) + \frac{1}{2}f\left((y_0, y_1)^0|s_3\right) \quad (36)$$

and decide in favor of hypothesis M_0 , i.e. $\hat{\text{M}}^0 = \text{M}_0$ if

$$\begin{aligned} &f((y_0, y_1)|\text{M}_0) > f((y_0, y_1)|\text{M}_1) \Leftrightarrow \\ &\quad e^{-\frac{2ab}{\sigma^2}} \sinh\left[(a+b)(y_0 - y_1)/\sigma^2\right] \\ &\qquad + e^{+\frac{2ab}{\sigma^2}} \sinh\left[(a-b)(y_0 - y_1)/\sigma^2\right] > 0. \quad (37) \end{aligned}$$

Thus, the receiver decides whether $\widehat{\text{M}}^0$ is M_0 or M_1 based on a pair of measurements $(y_0, y_1)^0$, where y_1 corresponds to the first half-bit and y_0 corresponds to the second half-bit of the previous bit. Similarly, the receiver decides whether $\widehat{\text{M}}^1$ is M_0 or M_1 based on a pair of measurements $(y_0, y_1)^1$ and Eq. (37), where y_0 corresponds to the second half-bit and y_1 corresponds to the first half-bit of the next bit. Finally, decision on tag A bit is made according to the following rule: if $\widehat{\text{M}}^0 = \widehat{\text{M}}^1$ (i.e. both are M_0 or both are M_1), then $\widehat{\text{tag}}_{\text{A}} = \text{“0”}$, otherwise $\widehat{\text{tag}}_{\text{A}} = \text{“1”}$.

It is again remarked that the above expressions require knowledge of σ^2 at the receiver. Simulation results show that the performance of the above detector practically coincides with the performance of Method 3 (Eq. (30)).

IV. Inventory Time Benefits

In this section, the impact of the above algorithms on the reduction of total inventory time (i.e. delay) for N tags is addressed in the context of framed Aloha. The latter as already mentioned forms the basis of commercial RFID protocols (e.g. Gen2). High SNR analysis follows, assuming that, when *exactly* one or two tags transmit in a given slot, their information can be correctly received. This section offers exact, closed-form formulas that compute the average inventory time and analysis results are validated by simulations.

In the basic version of framed Aloha, access is operated in frames where each frame is divided in L slots and tags at the beginning of each frame select independently and randomly one of the L slots to transmit their information. The beginning

of each slot is marked by transmission of appropriate messages from a central controller. At the end of the frame, the central controller (e.g. reader in the context of RFID applications) re-estimates the number of remaining tags and advertises a new number L of total slots for the next frame. The remaining tags select independently and randomly the slot they are going to transmit in the next frame and the process continues until a predetermined number of tags is accessed. It is remarked that for the particular case of Gen2 the number of slots per frame is set at $L = 2^Q$ and reader advertises Q at the beginning of each frame.

For a given number N of tag population and a number L of slots at a given frame, the probability of q tags transmitting at a given slot is described by the binomial term

$$\Pr(q)_{N,L} = \binom{N}{q} \left(\frac{1}{L}\right)^q \left(1 - \frac{1}{L}\right)^{N-q}. \tag{38}$$

Thus, successful transmission of tag information at a given slot can be readily calculated, also offering a measure of throughput.

First, it is assumed that tag collision occurs when *more than one* tags select the same slot, i.e. conventional processing at the reader. In that case, successful tag transmission occurs if *exactly one* tag transmits at a slot and the throughput per slot ρ_1, assuming detection at high SNR, is given by

$$\begin{aligned}\rho_1(N,L) &\triangleq \Pr(\text{slot success}) = \Pr(q=1)_{N,L} \\ &= N\left(\frac{1}{L}\right)\left(1-\frac{1}{L}\right)^{N-1}.\end{aligned} \tag{39}$$

Maximizing throughput per slot for a given number of slots L per frame offers the appropriate number of slots which, for the case of conventional reader processing, is equal to the number of tags:

$$\max_L \{\rho_1(N,L)\} \Rightarrow \widehat{L}_1(N) = N. \tag{40}$$

Second, for nonconventional reader processing, e.g. when exactly one out of two tags can be decoded at the event of simultaneous transmission of two tags (as described in Section III), the throughput per slot ρ_2, assuming detection at high SNR, is given by

$$\begin{aligned}\rho_2(N,L) &\triangleq \Pr(\text{slot success}) = \Pr(q=1)_{N,L} + \Pr(q=2)_{N,L} \\ &= \frac{N}{L}\left(1-\frac{1}{L}\right)^{N-1} + \binom{N}{2}\left(\frac{1}{L}\right)^2\left(1-\frac{1}{L}\right)^{N-2}.\end{aligned} \tag{41}$$

Notice that, if we assumed that *both* tags (and not just one out of two) could be decoded at the case of simultaneous transmission of exactly two tags, then a factor of 2 would multiply the second probability term above. Maximization of the above throughput quantity offers the appropriate choice for number of slots per frame:

$$\max_L \{\rho_2(N,L)\} \Rightarrow \widehat{L}_2(N) = 1 + \sqrt{1 + \frac{N(N-3)}{2}}. \tag{42}$$

Notice that, for $N < 3$ (i.e. $N = 1$ or $N = 2$), the appropriate number of slots is $\widehat{L}_2(N) = 1$, as expected.

The basic framed Aloha control algorithm works as follows: maximize slot throughput per frame, i.e. set $L(N) = \widehat{L}_j(N)$, depending on how *tag collision* is defined (whether the aforementioned detection algorithms of Section III are applied, in which case $j = 2$, or not, and thus $j = 1$). When frame is completed (i.e. all slots are tested), update number N of backlogged tags (remaining number of tags to be read) and start a new frame.

It is remarked that the above algorithm assumes that the central controller (e.g. reader) has acquired an accurate estimate of the total number of tags N. Such information can be inferred from the number of empty or collided slots and there are specific proposals in the literature, based on deterministic [9], probabilistic [23], [24], or recursive [25] techniques. More importantly, the above policy maximizes throughput per frame and not total number of frames (overall delay). It was recently shown that it could be beneficial to stop a frame before the total number of slots is tested (especially when probability of tag transmitting at remaining slots is small) and start a new frame with an updated slot number [26], [27]. Optimizing the framed Aloha policies are beyond the scope of this work.

The *expected* total number of frames F and *expected* total number of slots, required for the aforementioned basic framed Aloha scheme, can be readily calculated with the recursive equations (43)-(45) below, with initial condition $N(1) = \mathcal{N}$, where $\mathcal{N}$ denotes the total number of tags to be inventoried, index i denotes the frame number, and index j indicates whether the reader can detect one tag information out of two collided signals ($j = 2$) or not ($j = 1$):

$$L(i) = \widehat{L}_j(N(i)), \tag{43}$$

$$N(i+1) = N(i) - L(i)\ \rho_j(N(i), L(i)), \tag{44}$$

$$\sum_{i=1}^{F} L(i)\ \rho_j(N(i), L(i)) \geq a_p\ N. \tag{45}$$

Eq. (43) sets the number of slots per frame according to Eq. (40) or Eq. (42), depending on the reader detection method. Eq. (44) computes the expected number of remaining tags at the end of the frame, which is used to calculate the number of slots for the next frame. Eq. (45) sums all accessed tags and terminates the recursion if their sum is above the percentage a_p of the total tags that need to be read.

With the above recursion, the *expected* total number of frames F and slots per frame $L(i)$ are estimated, when Eq. (40) or Eq. (42) are utilized, according to the basic framed Aloha scheme described above. Simulation results in Section V confirm the recursive theoretical calculation above. In either cases, the *expected* total number of slots required to access $(a_p \times N)$ tags (e.g. $a_p = 100\% = 1$) is given by

$$\sum_{i=1}^{F} L(i). \tag{46}$$

With the above recursive methodology, inventory time benefits (i.e. delay reduction) can be readily calculated when detection techniques for two collided tags are utilized, as opposed to conventional detection (where collided signals of two tags are discarded). Additional analysis regarding variants of framed Aloha (e.g. Gen2) can be found in [15] and [28]. Finally, it is noted that the above methodology can be easily extended to cover the case of *three* (or more than three) tags

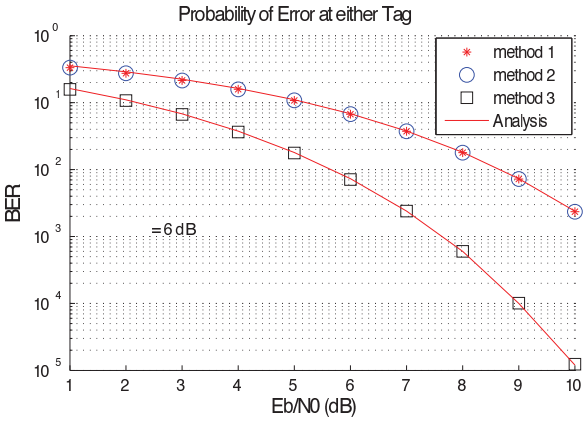

Fig. 6. BER at either tag vs SNR (fixed $\Psi = 6$dB).

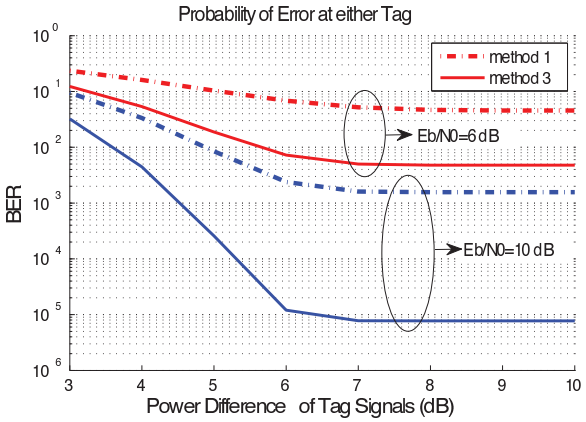

Fig. 7. BER at either tag vs tag power ratio Ψ (fixed SNR).

transmitting at the same slot and the reader being able to detect the strongest. However, the probability of three tags selecting the same slot in framed Aloha systems is in general smaller than the probability of two tags transmitting at the same slot and, thus, the observed benefits are not expected to be substantially better than the two-tag case [15].

V. Numerical Results

In the numerical results of this section, the signal-to-noise ratio (SNR) $E_b/N_0 = b^2/\sigma^2$ as well as the power ratio between the two baseband tag signals $\Psi = a^2/b^2$ are considered.

In Fig. 6, the BER as a function of SNR is depicted, when detection error at *either* tag (A or B) is considered. The power ratio between the two tags is set to $\Psi = 6$ dB (i.e. $a = 2b$) and Methods 1-3 (Subsections III-A-III-C) are tested (in Method 2, knowledge of noise variance σ^2 at the receiver is assumed). It is found that simulation matches analytical results of Method 1 (Eq. (8)) while Method 1 performs as well as Method 2. Such result could cause small surprise, given that Method 1 does not require any type of noise variance estimation. However, as already mentioned, Method 1 performs memoryless ML detection on half-bits with observations that offer sufficient statistics and, thus, its performance should not differ from Method 2 (which is also ML memoryless detection). It is noted however that Method 2 under imprecise knowledge of σ^2 offers deteriorated performance. Furthermore, simulation matches analysis results (Eq. (29)) for Method 3 which performs 3dB better than Method 1 due to intelligent exploitation of FM0 memory, as explained in Subsection III-C.

In Fig. 7, the previous experiments are repeated for Methods 1 and 3, with fixed SNR and variable Ψ. As Ψ increases, the overall BER reaches a plateau. That is due to the fact that error at either tag is considered and, thus, the depicted BER is limited by the weakest tag (B in our case); by increasing Ψ, errors at the strongest tag (tag A) are decreased but errors at the weakest tag are left unaffected. Thus, in cases where there is collision with a "weak" tag, the reader should only focus on the stronger tag.

Such strategy is examined in Fig. 8 where error only at tag A is considered and Methods 1-5 are tested for fixed Ψ and variable SNR. It can be seen that simulation matches analysis

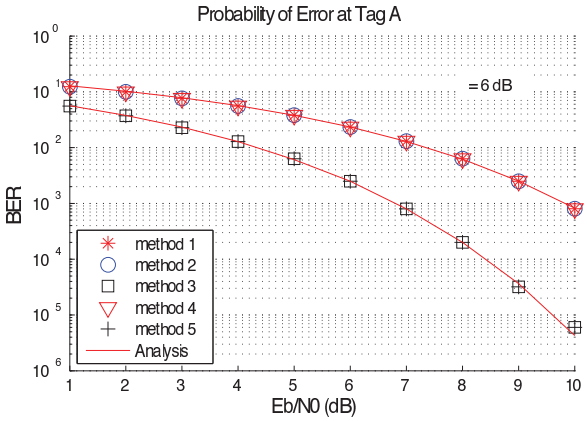

Fig. 8. BER at tag A only vs SNR (fixed $\Psi = 6$dB).

results for Method 1 (Eq. (11)) while Methods 2 and 4 perform no better than Method 1. Methods 2, 4, and 5 are assumed with perfect knowledge of noise variance σ^2. Fig. 8 shows that one could use Method 1 for single tag detection, when two tags collide, without any need for noise variance estimation and without performance loss, compared to the ML Method 4. A 3dB improvement can be further observed if Method 3 is utilized. Simulation results match analysis (Eq. (30)) for Method 3 which performs no worse than Method 5, even though the latter requires estimation of the noise variance σ^2 (assumed perfect in the depicted results).

Thus, Method 3 for single tag information extraction out of two collided tags offers a simple and effective scheme without requiring noise variance estimates by simple exploitation of FM0 memory. Fig. 9 repeats the aforementioned experiments for Methods 1 and 3 with variable Ψ and fixed SNR. It can be seen that Method 3 drops the BER to values on the order of 10^{-6} for SNR close to 10dB and $\Psi = 6$dB. One immediate question emerges: could additional FM0 memory (more than one bit) further reduce BER? The answer is negative and was already given by Simon and Divsalar for single-tag detection [16].

Finally, in Fig. 10, the expected total number of slots required to access N tags is depicted, with the basic framed Aloha scheme of Section IV. Simulation matches the analytical results of Eq. (46) through the recursive methodology in

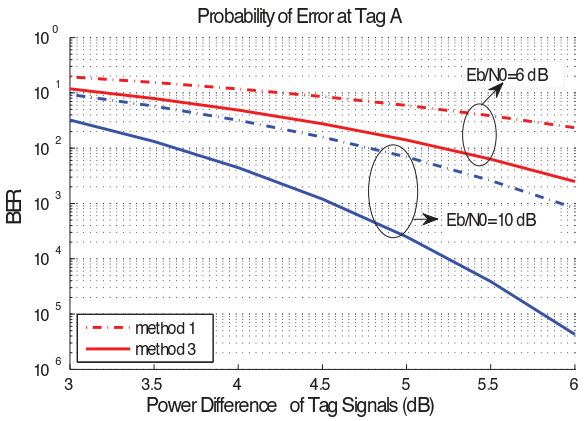

Fig. 9. BER at tag A only vs tag power ratio Ψ (fixed SNR).

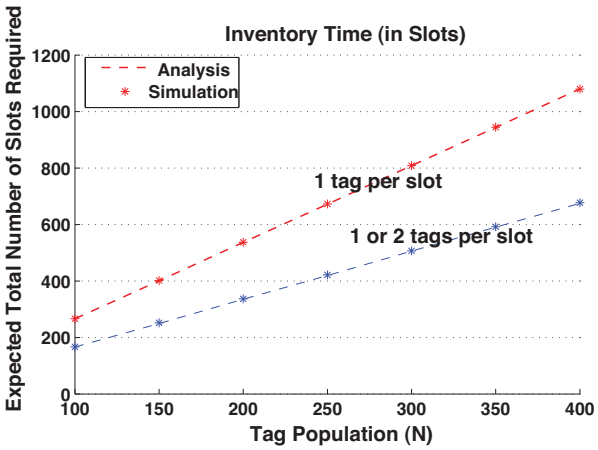

Fig. 10. Total number of required slots in framed Aloha as a function of tag population for different types of "collision."

Eqs. (43)-(45) for the whole population of tags (i.e $a_p = 1$). It can be seen that reader's ability to detect and extract information for one out of two collided tag signals can significantly reduce overall inventory time (i.e. total number of slots) by 40% (and even more for higher tag population N), depending on the total number of tags. Additional results relevant to inventory time reduction in a basic version of Gen2 (which is also a version of framed Aloha) can be found in [28].

VI. Conclusion

Commercial RFID protocols based on framed Aloha, including Gen2, can substantially benefit from the methodology of this work. What is needed is simple augmentation of detection algorithms at the reader, alongside the lines of this work. Single-bit memory-assisted algorithms are the basis of two-tag detection that could lead to inventory time reduction of N tags on the order of 40% under certain conditions (e.g. high-SNR, sufficient tag signal separation Ψ) for basic framed Aloha access schemes without modification of reader RF front end. The algorithms could be of importance to single-antenna (e.g. portable) readers as well as multiple-antenna readers (in antenna-switching mode).

References

[1] H. Stockman, "Communication by means of reflected power," *Proc. IRE*, pp. 1196–1204, 1948.
[2] K. Finkenzeller, *RFID Handbook: Fundamentals and Applications in Contactless Smart Cards and Identification*, 2nd edition. John Wiley and Sons, 2003.
[3] G. Vannucci, A. Bletsas, and D. Leigh, "A software-defined radio system for backscatter sensor networks," *IEEE Trans. Wireless Commun.*, vol. 7, no. 6, pp. 2170–2179, June 2008.
[4] A. Bletsas, S. Siachalou, and J. N. Sahalos, "Anti-collision backscatter sensor networks," *IEEE Trans. Wireless Commun.*, vol. 8, no. 10, pp. 5018–5029, Oct. 2009.
[5] C. M. Kruesi, R. J. Vyas, and M. M. Tentzeris, "Design and development of a novel 3D cubic antenna for wireless sensor networks (WSN) and RFID applications," *IEEE Trans. Antennas Propag.*, vol. 57, no. 10, pp. 3293–3299, Oct. 2009.
[6] J. Paradiso, K. Hsiao, and A. Benbasat, "Tangible music interfaces using passive magnetic tags," in *Proc. 2001 ACM Conf. Human Factors Computing Systems: Special Workshop New Interfaces Musical Expression*.
[7] J. Paradiso, L. Pardue, K. Hsiao, and A. Benbasat, "Electromagnetic tagging for electronic music interfaces," *J. New Music Research*, vol. 32, no. 4, pp. 395–409, Dec. 2003.
[8] EPC Radio-Frequency Identity Protocols, Class-1 Generation-2 UHF RFID Protocol for Communications at 860 MHZ-960 MHZ, Version 1.2.0, EPC Global, 2008.
[9] F. C. Schoute, "Dynamic frame length ALOHA," *IEEE Trans. Commun.*, vol. 31, no. 4, pp. 565–568, Apr. 1983.
[10] J. E. Wieselthier, A. Ephremides, and L. A. Michaels, "An exact analysis and performance evaluation of framed ALOHA with capture," *IEEE Trans. Commun.*, vol. 31, no. 2, pp. 125–137, Feb. 1989.
[11] G. R. Woo, "Demonstration and evaluation of co-channel DBPSK source separation," M.S. thesis, MIT, 2007.
[12] D. Shen, G. Woo, D. P. Reed, A. B. Lippman, and J. Wang, "Separation of multiple passive RFID signals using software defined radio," in *Proc. 2009 IEEE RFID Conf.*.
[13] C. Angerer, R. Langwieser, and M. Rupp, "RFID reader receivers for physical layer collision recovery," *IEEE Trans. Commun.*, vol. 58, no. 12, pp. 3526–3537, Dec. 2010.
[14] A. F. Mindikoglu and A.-J. van der Veen, "Separation of overlapping RFID signals by antenna arrays," in *Proc. 2008 IEEE ICASSP*, pp. 2737–2740.
[15] B. Frey, "Source separation for UHF RFID," M.S thesis, Delft and ETH, 2008.
[16] M. Simon and D. Divsalar, "Some interesting observations for certain line codes with application to RFID," *IEEE Trans. Commun.*, vol. 54, no. 4, pp. 583–586, Apr. 2006.
[17] M. Buettner and D. Wetherall, "A "Gen 2" RFID monitor based on the USRP," *ACM SIGCOMM Computer Commun. Review*, vol. 40, no. 3, pp. 42–47, July 2010.
[18] D. M. Dobkin, *The RF in RFID: Passive UHF RFID in Practice*. Newnes (Elsevier), 2008.
[19] G. J. M. Janssen, "Dual-signal receiver structures for simultaneous reception of two BPSK modulated co-channel signals using signal cancellation," *Wireless Pers. Commun.*, vol. 1, pp. 43–59, 1994.
[20] R. S. Khasgiwale, R. U. Adyanthaya, and D. W. Engels, "Extracting information from tag collisions," in *Proc. 2009 IEEE RFID Conf.*
[21] A. Dimitriou, A. Bletsas, and J. Sahalos, "Room coverage improvements in UHF RFID with commodity hardware," *IEEE Antennas Propag. Mag.*, vol. 53, no. 1, Feb. 2011.
[22] A. Bletsas, A. G. Dimitriou, and J. N. Sahalos, "Improving backscatter radio tag efficiency," *IEEE Trans. Microw. Theory Tech.*, vol. 58, no. 6, pp. 1502–1509, June 2010.
[23] H. Vogt, "Efficient object identification with passive RFID tags," in *PERVASIVE 2002* (Lecture Notes in Computer Science (LNCS)), F. Mattern and M. Naghshineh, editors. Zurich, Switzerland: Aug. 2002, vol. 2414.
[24] C. Floerkemeier, "Bayesian transmission strategy for framed ALOHA based RFID protocols," in *Proc. 2007 IEEE RFID Conf.*.
[25] J.-B. Eom and T.-J. Lee, "Accurate tag estimation for dynamic framed-slotted ALOHA in RFID systems," *IEEE Commun. Lett.*, vol. 14, no. 1, pp. 60–62, Jan. 2010.
[26] L. Zhu and T.-S. P. Yum, "Design and analysis of framed ALOHA based RFID anti-collision algorithms," in *Proc. 2009 IEEE Global Telecommun. Conf.*
[27] ——, "Optimal framed ALOHA based anti-collision algorithms for RFID systems," *IEEE Trans. Commun.*, vol. 58, no. 12, pp. 3583–3592, Dec. 2010.

[28] J. Kimionis, A. Bletsas, A. G. Dimitriou, and G. N. Karystinos, "Inventory time reduction in Gen2 with single-antenna separation of FM0 RFID signals," in *Proc. 2011 IEEE Int. Conf. RFID Technologies Applications*, pp. 494–501.

Aggelos Bletsas (S'03-M'05) received, with excellence, his diploma degree in electrical and computer engineering from Aristotle University of Thessaloniki, Greece, in 1998 and the S.M. and Ph.D. degrees from the Massachusetts Institute of Technology in 2001 and 2005, respectively. He worked at Mitsubishi Electric Research Laboratories (MERL), Cambridge, MA, as a Postdoctoral Fellow and at the Radiocommunications Laboratory (RCL), Department of Physics, the Aristotle University of Thessaloniki, as a visiting scientist. He joined the Electronic and Computer Engineering Department, Technical University of Crete, in the summer of 2009, as an Assistant Professor. His research interests span the broad area of scalable wireless communication and networking, with emphasis on relay techniques, signal processing for communication, radio hardware/software implementations for wireless transceivers and low cost sensor networks, RFID, time/frequency metrology, and bibliometrics. Dr. Bletsas was the co-recipient of the IEEE Communications Society 2008 Marconi Prize Paper Award in Wireless Communications, best paper distinction in ISWCS 2009, Siena, Italy, and Second Best Student Paper Award in the IEEE RFID-TA 2011, Sitges, Barcelona, Spain.

John Kimionis (S'10) received his diploma degree in electronic and computer engineering from the Technical University of Crete, Greece, in 2011, and is currently a M.Sc. candidate and research assistant at the ECE department, Technical University of Crete. His research interests are in the areas of backscatter radio and RFID, wireless sensor networks, software defined radio for backscatter and sensor networks, microwave/RF engineering, and telecom hardware/embedded systems development. He has received fellowship awards for his undergraduate and graduate studies, and was the recipient of the Second Best Student Paper Award in the IEEE International Conference on RFID-Technologies and Applications (RFID-TA) 2011, Sitges, Barcelona, Spain.

Antonis G. Dimitriou (S'01-M'07) received the diploma and the Ph.D degree in electrical and computer engineering from the Aristotle University of Thessaloniki (AUTh), Greece, in 2001 and 2006, respectively. Since 2007, he has been with the Department of Electrical and Computer Engineering of AUTh. Since 2001, he has participated in 18 research projects in the fields of communications, antennas, propagation, signal processing, and RFIDs, including the design of a DCS-1800 cellular network that operated within the Olympic Stadium during the 2004 Olympic Games, and a pilot implementation of an RFID system in a hospital in Nicosia. He is the author or co-author of approximately 35 journal and conference papers. His current interests are in the areas of electromagnetic-wave propagation, planning and optimization of wireless networks, and relay techniques in wireless communications and RFIDs. Dr. Dimitriou was the recipient of the Ericsson Award of Excellence in Telecommunications for the best undergraduate thesis in 2001.

George N. Karystinos (S'98-M'03) was born in Athens, Greece, on April 12, 1974. He received the Diploma degree in computer science and engineering (five-year program) from the University of Patras, Patras, Greece, in 1997 and the Ph.D. degree in electrical engineering from the State University of New York at Buffalo, Amherst, NY, in 2003. In August 2003, he joined the Department of Electrical Engineering, Wright State University, Dayton, OH, as an Assistant Professor. Since September 2005, he has been an Assistant Professor with the Department of Electronic and Computer Engineering, Technical University of Crete, Chania, Greece. His current research interests are in the general areas of communication theory and adaptive signal processing with an emphasis on wireless and cooperative communications systems, low-complexity sequence detection, optimization with low complexity and limited data, spreading code and signal waveform design, and sparse principal component analysis.

Dr. Karystinos received a 2001 IEEE International Conference on Telecommunications best paper award, the 2003 IEEE Transactions on Neural Networks Outstanding Paper Award, and the 2011 IEEE International Conference on RFID-Technologies and Applications Second Best Student Paper Award. He is a member of the IEEE Communications, Signal Processing, Information Theory, and Computational Intelligence Societies and a member of Eta Kappa Nu.